130 KIEE International Transactions on PE, Vol. 3-A No. 3, pp. 130~138, 2003

A Novel Detection Technique for Voltage Sag in Distribution Lines Using the Wavelet Transform

Young-Hun Ko*, Chul-Hwan Kim and Sang-Pil Ahn*****

Abstract - This paper presents a discrete wavelet transform approach for determining the beginning and end times of voltage sags. Firstly, investigations in the use of some typical mother wavelets, namely Daubechies, Symlets, Coiflets and Biorthogonal are carried out and the most appropriate mother wavelet is selected. The proposed technique is based on utilizing the maximum value of D1 (at scale 1) coefficients in multiresolution analysis (MRA) based on the discrete wavelet transform. The results are compared with other methods for determining voltage sag duration, such as the Root Mean Square (RMS) voltage and Short Time Fourier Transform (STFT) methods. It is shown that the voltage sag detection technique based on the wavelet transform is a satisfactory and reliable method for detecting voltage sags in power quality disturbance analysis.

Keywords: Multiresolution Analysis, Power Quality, Voltage Sag, Wavelet Transform

1. Introduction

Electric power quality has become an important issue in the power systems of today. The demand for "clean power" has increased over the past several years due to the increased use of microelectronic processors in various types of equipment, such as computer terminals, programmable logic controllers (PLCs), diagnostic systems, etc. Most of these devices are susceptible to disturbances on the incoming alternating voltage waveform. Thus, to ensure efficient and proper utilization of sensitive load equipment, a clean voltage waveform is vitally important. The most common type of power quality disturbance encountered at the distribution level is voltage sag. Because of the increased use of sensitive electronic equipment, these disturbances have a greater impact on customers than ever before. As a result, monitoring and assessment of the system performance at both the transmission and distribution voltage levels are becoming increasingly important [1- 5].

The first notion for utilizing the wavelet theory in power systems is credited to Ribeiro [6]. Wavelet theory uses special functions called mother wavelets. There are an abundance of mother wavelets and the selection of a wavelet will depend on a particular application. Thus, initial selection of the appropriate mother wavelet is essential in order to enhance the performance of specific applications. In addition, much of the power system analysis is steady state. However, in the area of electric power quality analysis, transients may take on an important role [7 - 13]. By using the multiresolution analysis (MRA) technique, the power quality disturbance signal is divided into two subsidiary signals; one being the smoothed version of the Power Quality (PQ) disturbance signal, and the other being the detailed version of the PQ disturbance signal containing sharp edges, transitions and jumps. In this respect, the MRA technique allows detection of sharp time changes in voltage signal such as voltage sags, interruptions, overvoltages, and transients. Because of this particular attribute, applications of the MRA technique to PQ disturbance detection are increasing [14]. In this paper, the MRA technique based on the wavelet transform is applied to voltage sag detection.

As mentioned before, an important pre-requisite to the work described herein is the selection of the most appropriate mother wavelet, particularly in view of the fact that the performance of the voltage sag detection technique is heavily dependent upon the type of mother wavelet chosen. This paper then describes a novel detection technique for voltage sags caused by change of linear loads in distribution lines; it essentially determines the beginning and end times of voltage sags utilizing the maximum value of D1 coefficients via MRA based on the discrete wavelet transform.

The results attained are compared with other traditional methods such as those based on RMS voltage and STFT technology and the effectiveness of the technique developed herein is illustrated by considering an IEEE 13-bus distribution system [15]; the system simulation includes a voltage sag model using the electromagnetic transients program (EMTP).

* Product R&D center in Daewoo Computer, Korea. (yhko@dwsolo.co.kr)
** School of Information & Communication Engineering, Sungkyunkwan University, Korea. (chkim@skku.edu)
*** Korea Electrotechnology Research Institute, Korea. (spahn@keri.re.kr)
Received April 18, 2003 ; Accepted July 1, 2003

2. Basic Principle of Voltage Sags

2.1 Fundamentals of Voltage Sags

Voltage sag is defined as a momentary decrease of between 0.1 and 0.9 p.u. in the RMS voltage magnitude for durations from 0.5 to 30 cycles, usually caused by a remote fault somewhere within the power system. Voltage sag is the most important PQ problem facing industrial customers. Equipment used in modern industrial plants (process controllers, programmable logic controllers, adjustable speed drives, robotics) is actually becoming more sensitive to voltage sags as the complexity of the equipment increases. Even relays and contactors in motor starters can be sensitive to voltage sags, resulting in shutdown of a process when they drop out. As an example, Fig. 1 typifies a voltage sag disturbance.

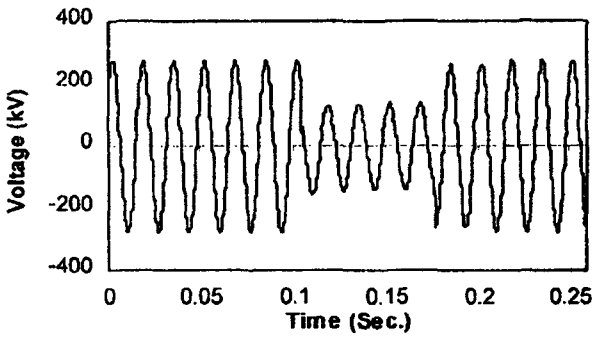

Fig. 1 Typical waveform of voltage sag

Voltage sags are typically caused by fault conditions. Utility system faults can occur in a distribution system or in a transmission system. A fault on one feeder will cause an interruption, which will affect the customers on that particular feeder. However, most of the customers on the other parallel feeders will also experience voltage sag while the fault is actually on the system. Faults on a transmission system can affect an even greater number of customers. Customers hundreds of miles from the fault location can still experience voltage sags resulting in equipment maloperation when the fault is on the transmission system. Motor starting can also result in undervoltages, but these are typically longer in duration than 30 cycles and associated magnitudes are not as low. Motor starting voltage variations are often referred to as voltage flicker, especially if the motor starting occurs frequently.

2.2 Specified Voltage Method

This section explains current methods employed in most existing voltage sag monitors. Since a voltage sag disturbance is defined as a reduction in the RMS voltage magnitude for a given range of time, it follows that one way to define the sag duration is by looking for RMS voltage levels that drop below a specified threshold. The RMS voltage may be calculated from digitally sampled data using a one-cycle window by (1) [5].

$$V_i^{rms} = \sqrt{\frac{1}{N}\sum_{j=i}^{i+N-1} V_j^2} \quad (1)$$

Where N is the number of sample points per cycle of fundamental, V_j is the j^{th} sample of the recorded voltage waveform, and V_i^{rms} is the i^{th} sample of the calculated RMS voltage. The start and stop times of the sag can be defined in a number of ways, depending on the chosen RMS voltage thresholds. The start time is taken as the first point where V^{rms} drops below 0.95 p.u. To identify the end time, a search is conducted for an interval whereby V^{rms} recovers to 0.96 p.u. for at least half a cycle.

This method is very straightforward, but not necessarily very accurate. Since the RMS voltage is in effect a moving average calculated using a one-cycle window, there can be a lag of up to one cycle from the time the voltage sag actually starts (or clears) and the time that the RMS voltage falls below the given threshold. Furthermore, since the actual fault inception and clearing times are not accurately determined, one cannot use the results in a realistic assessment.

3. Multiresolution Analysis (MRA)

The wavelet transform normally consists of the analysis and synthesis wavelet pair. Synthesis is used for waveform reconstruction. In the analysis process, a given signal is separated into its constituent wavelet sub-bands or levels. Each of these levels represents a part of the original signal occurring at a particular time and in a particular frequency band. These individual bands tend to be of uniform width with respect to the log of their frequencies, as opposed to the uniform frequency widths of the Fourier spectral bands. In the common dyadic decomposition (to be used later), the sub-bands are represented by a frequency octave. These divided signals possess the powerful time-frequency localization property, which is one of the major attributes of the wavelet transform; that is, the resulting broken down signals can then be analyzed in both time and frequency domains.

Multiresolution analysis refers to the procedures to obtain lowpass approximations and bandpass details from the original signals. An approximation is a low resolution representation of the original signal, while a detail is the difference between two successive low resolution representations of the original signal. An approximation contains the general trend of the original signal, while a detail embodies

the high frequency contents of the original signal. Approximations and details are obtained through a succession of convolution processes. The original signal is divided into different scales of resolution, rather than different frequencies, as is the case in Fourier analysis.

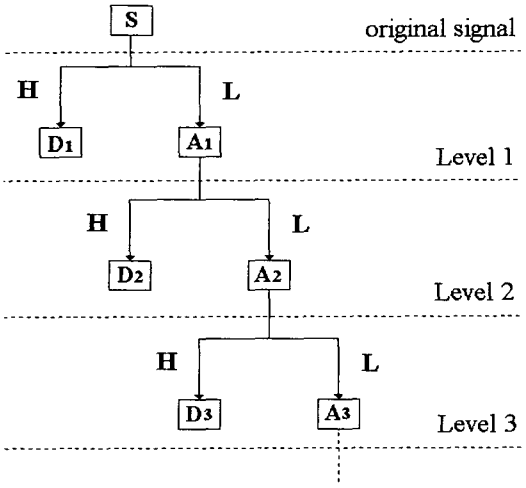

L: lowpass filter, H: highpass filter
A1, A2, A3: approximations of the original signal at levels 1, 2 and 3 respectively.
D1, D2, D3: details of the original signal at levels 1, 2 and 3 correspondingly.

Fig. 2 Multiresolution analysis

The algorithm of multiresolution decomposition is illustrated in Fig. 2, where 3 levels of decomposition are taken as an example for illustration. The details and approximations of the original signal S are obtained by passing it through a filter bank, which consists of lowpass and highpass filters. A lowpass filter smoothes out the high frequency components, while the highpass filter picks out the high frequency contents in the signal being analyzed. With reference to Fig. 2, the multiresolution decomposition procedures are defined as in (2)

$$D_j(n) = \sum_k h(k) A_{j-1}(n-k)$$
$$A_j(n) = \sum_k l(k) A_{j-1}(n-k) \quad (2)$$

where l, h are lowpass and highpass filter vectors, D_j and A_j are the detail and approximation at resolution j, j=1,2,...,J, A_{j-1} are the approximation of the level immediately above level j, k=1,2,...,K, K is the length of the filter vector.

4. Detection Technique of Voltage Sags Using the Wavelet Transform

4.1 System Model Studied

For illustration purposes, an unbalanced distribution system corresponding to the IEEE 13-bus distribution test system has been adopted as depicted in Fig. 3. This system consists of a three-phase primary feeder with three-, two- and single-phase laterals. It includes both overhead open-wire lines and underground cables. The substation transformer serving this feeder is 5000 kVA and the three-phase short circuit MVA on the 115 kV bus of the substation is 1100. Loads consist of three-phase motor loads and single-phase loads [15].

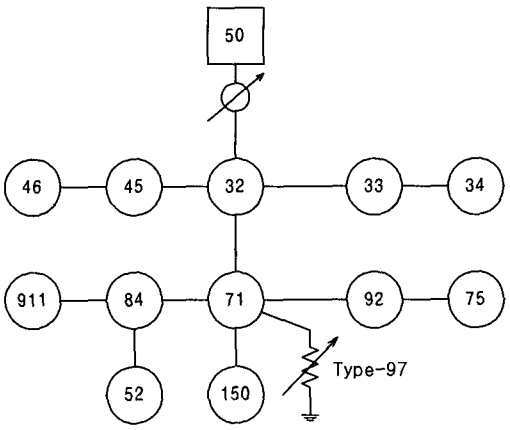

Fig. 3 IEEE 13-bus test system

Modeling of voltage sags is implemented through the EMTP's subsection TACS (Transient Analysis of Control Systems), in which type-97 staircase time-varying resistance is connected to bus 71. The simulation of the power system has been carried out using the well-known EMTP software. The number of data sets with voltage sags applied to this simulation is 20 (caused by a change in the linear load) and are listed in Table 1.

Table 1. Data cases of voltage sags

Case #	Start time [msec]	End time [msec]	Duration time[cycle]	Resistance [ohm]
1	296.4	440.3	8.634	23
2	195.4	330.3	8.093	19
3	93.9	404.3	18.624	12
4	121.4	221.9	6.030	23
5	175.8	361.9	11.166	33
6	331.1	427.3	5.772	35
7	231.1	427.3	11.772	15
8	189.9	421.2	13.878	44
9	142.8	404.5	15.702	49
10	193.8	312.5	7.122	27
11	73.1	245.5	10.344	39
12	144.0	395.4	15.084	16
13	224.2	371.4	8.832	29
14	129.2	403.4	16.452	39
15	258.8	391.3	7.950	31
16	281.4	444.5	9.786	21
17	210.0	412.5	12.150	41
18	256.7	352.4	5.742	17
19	160.3	441.5	16.872	28
20	237.8	350.2	6.744	37

Table 2 Results of detection using various mother wavelets

Mother wavelet	N	Avg. error of Estimated start time [cycle]	Avg. error of estimated end time [cycle]
Daubechies	2	0.4695	0.0563
	4	0.0424	0.0361
	6	0.0511	0.0421
	8	0.4636	0.0488
	10	0.0499	0.0479
Symlets	2	0.4695	0.0540
	3	0.0488	0.0358
	4	0.0511	0.0398
	5	0.0414	0.5029
	6	0.0511	0.0428
	8	0.0538	0.0421
Coiflets	2	0.0511	0.0375
	3	0.0538	0.0421
	4	0.0538	0.0421
	5	0.0566	0.0431
Biorthogonal	1.3	2.2360	4.0520
	2.6	0.0511	0.0370
	3.1	0.0419	0.0383
	4.4	0.0511	0.0453

4.2 Selection of Mother Wavelet for Detection of Voltage Sags

In the detection technique for voltage sags, selection of the most appropriate mother wavelet is essential to enhance the performance of the technique by rapid extraction of useful information. In this paper, a total of 20 mother wavelets based on Daubechies (dbN), Symlets (SymN), Coiflets (CoifN) and Biorthogonal (BiorN) were considered and the performances of the various voltage sag techniques were then compared. It should be noted that 'N' signifies the order of the filter adopted. With regard to the selection of the mother wavelet, the simple criterion adopted herein is the least average error relating to the start and end times. The resultant novel detection technique for voltage sags will be described in the next section.

Table 2 shows results of the detection using various mother wavelets. When considering the error at the start time, sym5, bior3.1, db4, sym3 and db10 provide the minimum error and likewise, for the end time, any one of the mother wavelets, sym3, db4, coif2, bior2.6 and bior3.1 are appropriate. For this study, the tested db4 mother wavelet was chosen.

4.3 Detection Techniques for Voltage Sags

4.3.1 Detection algorithm for voltage sags using STFT

Fig. 4 shows the detection algorithm using the STFT, where i and j are sample numbers and V_60 is voltage of fundamental component (60Hz). Threshold c is used to determine whether the magnitude of voltage is in the range of the defined voltage sags. As can be seen, when the voltage of fundamental component at i^{th} sample number is less than the threshold c, the time is set to the beginning, i.e. T1. After that, j is incremented and T2, the end time is determined if V_60(j) is greater than threshold c. Finally, voltage sag can be ascertained by means of checking the duration, T2-T1. The optimal setting for c is 3.625, which can be derived from the voltage variation of fundamental frequency in all cases of voltage sags studied as shown in Fig. 7a. The setting value of this threshold is dependent on the application environments.

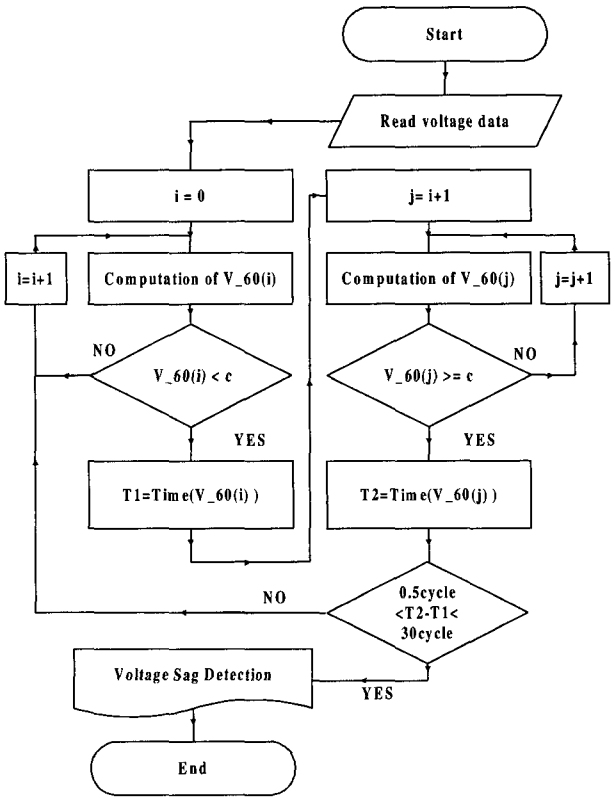

Fig. 4 Detection algorithm using STFT

4.3.2 Detection algorithm for voltage sags using RMS voltage

Detection algorithm using RMS voltage is shown in Fig. 5, where T is 64 samples. All procedures are similar to that of STFT, except that RMS values of voltages are used. Those RMS values are calculated over a 1-cycle period and the sampling rate employed is 3840 Hz i.e., 64 samples/cycle at 60Hz. The entire process is based on a moving window approach whereby the 1-cycle window is moved continuously by 1 sample. Therefore this process is different from previous voltage methods as mentioned in section 2.2.

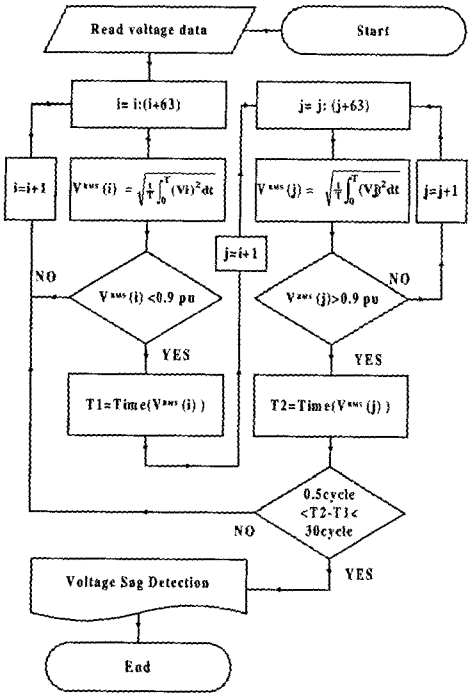

Fig. 5 Detection algorithm using RMS voltage

4.3.3 Detection algorithm for voltage sags using the wavelet transform

Fig. 6 shows the detection algorithm using the wavelet transform of the proposed technique, where T is 64 samples. In this algorithm, 1 level of multiresolution analysis (MRA) is taken to obtain the detail and approximations of the voltage signal. The approximation smoothes out the high frequency components, while the detail picks out the high frequency components (transient) in the voltage sags. Hence, two maximum values of D1 coefficients are utilized to determine the beginning and end times, respectively. Next to this MRA process, duration and magnitude conditions are checked similar to previous algorithms, except that A1 coefficients are utilized to calculate the RMS variation.

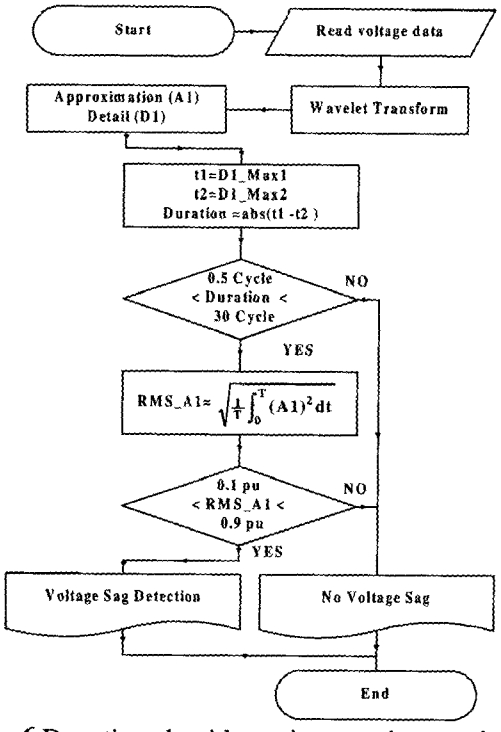

Fig. 6 Detection algorithm using wavelet transform

5. Simulation Results

The input voltage waveforms including voltage sags are modified by the capacitor voltage transformer (CVT), anti-aliasing lowpass filters and A/D conversion processes. It should be noted that although not shown here, response/limitations due to CVTs, relay hardware (such as voltage interface module comprising anti-aliasing filters and analogue-to-digital converters) and etc. have been taken into account in the simulation so that the performance of the detection technique attained pertains closely to that expected in reality.

5.1 Results of Detection using STFT

Voltage sags are analyzed by STFT and the results are depicted in Fig. 7. Figs. 7a, 7b, 7c, and 7d show the voltage variation of fundamental, 3rd, 5th, and 7th harmonic components in voltage waveforms respectively. It should be mentioned that although not shown here, voltage variation of the DC and 'even' harmonic components are also ana lyzed by the STFT. Since there are no specific characteristics in both 'odd' and 'even' harmonic components, only

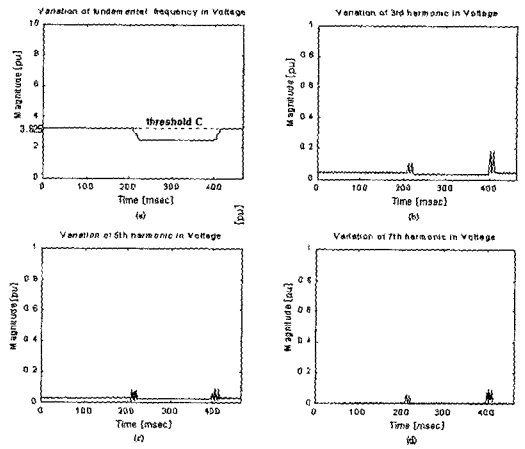

Fig. 7 Voltage variation of the fundamental, 3rd, 5th and 7th harmonic components
(a) Variation of fundamental frequency
(b) Variation of 3rd harmonic
(c) Variation of 5th harmonic
(d) Variation of 7th harmonic

Table 3 Results of detection using STFT

Case #	Start time		End time		Duration time [cycle]
	Estimated time [msec]	Error [cycle]	Estimated time [msec]	Error [cycle]	
1	298.6	0.1345	439.1	0.0638	8.429
2	196.7	0.0687	330.9	0.0419	8.054
3	94.7	0.0498	404.8	0.0287	18.605
4	121.7	0.0195	222.7	0.0539	6.056
5	176.9	0.0681	364.2	0.1365	11.238
6	331.9	0.0575	428.7	0.0918	5.806
7	232.0	0.0543	428.7	0.0918	11.800
8	190.4	0.0374	422.5	0.0760	13.923
9	143.6	0.0514	405.8	0.0755	15.733
10	194.6	0.0531	313.2	0.0413	7.117
11	73.9	0.0029	247.7	0.1328	10.426
12	144.6	0.0359	396.5	0.0596	15.109
13	224.8	0.0229	372.5	0.0744	8.866
14	130.1	0.0510	404.8	0.0755	16.482
15	260.1	0.0864	392.3	0.0595	7.929
16	282.0	0.0403	445.4	0.0456	9.802
17	211.2	0.0692	414.1	0.0914	12.175
18	258.1	0.0863	353.8	0.0894	5.744
19	161.2	0.0520	444.3	0.1702	16.982
20	238.3	0.0233	352.7	0.1518	6.868
	Avg. error	0.0532 [cycle]	Avg. error	0.0826 [cycle]	

Table 4 Results of detection using RMS voltage

Case #	Start time		End time		Duration time [cycle]
	Estimated time [msec]	Error [cycle]	Estimated time [msec]	Error [cycle]	
1	302.3	0.3566	435.9	0.2546	9.000
2	202.3	0.4094	326.8	0.2026	18.473
3	110.2	0.9778	393.0	0.6799	17.953
4	127.1	0.3398	218.8	0.1818	6.484
5	178.6	0.1731	360.7	0.0746	11.906
6	335.4	0.2662	426.6	0.0371	6.453
7	237.5	0.3816	420.8	0.3808	11.984
8	193.5	0.2214	419.5	0.1001	14.547
9	145.6	0.1699	402.9	0.1017	16.422
10	200.5	0.4092	310.7	0.1106	7.594
11	76.6	0.2102	244.0	0.0858	11.031
12	152.0	0.4826	392.4	0.1807	15.406
13	227.3	0.1778	369.3	0.1205	9.500
14	134.9	0.3405	402.3	0.0706	17.031
15	261.7	0.1811	386.7	0.2749	8.484
16	285.9	0.2770	443.2	0.0823	10.422
17	213.5	0.2077	410.9	0.1009	12.828
18	261.7	0.3059	349.7	0.1535	6.266
19	166.9	0.3904	436.7	0.2856	17.172
20	243.5	0.3354	345.3	0.2945	7.094
	Avg. error	0.3307 [cycle]	Avg. error	0.1887 [cycle]	

the fundamental component in voltage is adopted for the detection algorithm for voltage sags using the STFT. Table 3 shows the results of the detection using STFT, where all voltage sags can be detected within the least error. Average errors of estimated start and end times are 0.053 cycle and 0.083 cycle, respectively.

5.2 Results of Detection using RMS Voltage

Fig. 8a shows waveform of voltage sag and Fig. 8b shows the corresponding RMS variation of voltage sag in case study #7 shown in Table 1. In Fig. 8, the estimated start and end times are 237.5 msec and 420.8 msec, respectively. Estimated duration is 12 cycles. Table 4 shows the results of detection using RMS voltage, where all voltage sags can be detected, but average errors are slightly higher than those attained when the STFT is employed. Average errors of estimated start and end times are 0.331 cycle and 0.189 cycle, respectively.

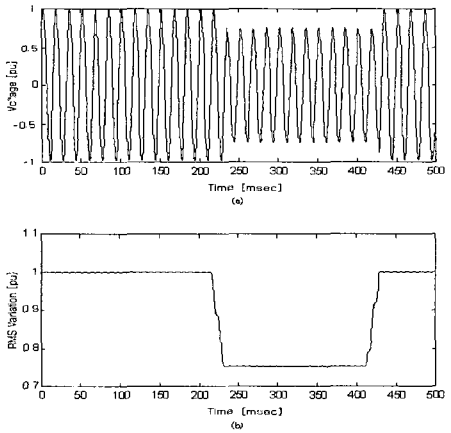

Fig. 8 Waveforms of voltage sag and RMS variation of voltage sags
(a) Waveform of voltage sag
(b) RMS variation of voltage sag

5.3 Results of Detection Using the Wavelet Transform

Fig. 9 shows the results of 4 levels of multiresolution analysis by db4 mother wavelet, Fig 9a being the input waveform of voltage sag in case study #10 shown in Table 1. Fig. 9b is the A1 coefficient and Figs. 9c, 9d, 9e, and 9f are D1, D2, D3, and D4 coefficients, respectively. Among these coefficients, D1 demonstrates a slightly better performance in the detection process than D2. Also, with respect to the speed of multiresolution analysis, the D1 coefficient in level 1 is slightly superior. However, in view of the fact that the utilization of the D2 coefficients for detecting voltage sags under faults is far superior than the employment of D1 (as shown later), maximum values based on D2 coefficients are applied in the detection algorithm of voltage sags using the wavelet transform in this paper. Table 5 shows the results of detection using the wavelet transform, where all voltage sags can be detected with the least error. Average errors of estimated start and end times are 0.042 cycle, 0.036 cycle respectively.

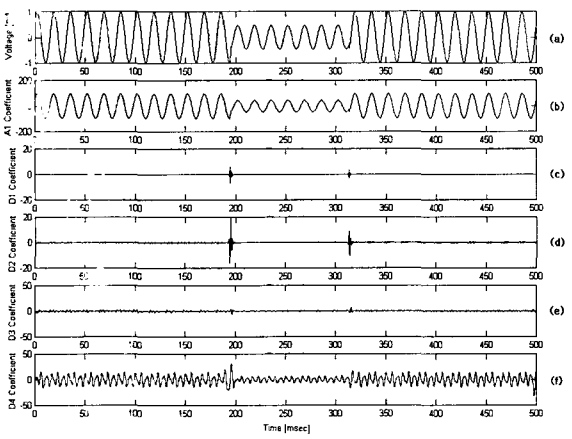

Fig. 9 Results of 4 levels of MRA by db4 mother wavelet
(a) Waveform of voltage sag
(b) A1 coefficient
(c) D1 coefficient
(d) D2 coefficient
(e) D3 coefficient
(f) D4 coefficient

Table 5 Results of detection using wavelet transform

Case #	Start time		End time		RMS of A1 coeffs. [pu]	Duration time [cycle]
	Estimated time [msec]	Error [cycle]	Estimated time [msec]	Error [cycle]		
1	297.1	0.0441	441.1	0.0579	0.536	8.641
2	196.1	0.0344	327.7	0.0151	0.624	8.016
3	94.5	0.0403	403.9	0.0236	0.878	18.562
4	121.9	0.0273	221.1	0.0412	0.536	5.953
5	176.6	0.0482	361.2	0.0433	0.396	11.078
6	332.0	0.0631	427.8	0.0381	0.376	5.781
7	231.8	0.0378	427.8	0.0381	0.748	11.797
8	190.6	0.0495	420.8	0.0220	0.307	13.182
9	143.5	0.0449	403.9	0.0392	0.279	15.625
10	194.5	0.0499	311.7	0.0481	0.469	7.031
11	73.7	0.0383	246.4	0.0549	0.342	10.359
12	144.5	0.0295	396.4	0.0536	0.713	15.109
13	225.0	0.0372	370.8	0.0268	0.442	8.750
14	129.7	0.0281	402.9	0.0393	0.342	16.391
15	259.6	0.0561	390.6	0.0405	0.418	7.859
16	282.3	0.0583	445.6	0.0583	0.577	9.797
17	210.7	0.0358	412.0	0.0384	0.327	12.078
18	257.6	0.0559	353.1	0.0495	0.681	5.734
19	160.9	0.0311	441.1	0.0201	0.455	16.812
20	238.5	0.0385	351.0	0.0493	0.358	21.062
	Avg. error	0.0424 [cycle]	Avg. error	0.0361 [cycle]		

5.4 Comparison of Results by Proposed Detection Algorithms

Fig. 10 depicts the estimated error of the start time in all simulation cases by the three proposed detection algorithms, and Fig. 11 also depicts the estimated error of the end time. With respect to the start time, total average errors in STFT, RMS voltage and wavelet transform are 0.053 cycle, 0.331 cycle and 0.042 cycle, respectively, and in the case of the end time, total average errors in STFT, RMS voltage and wavelet transform are 0.083 cycle, 0.189 cycle, and 0.036 cycle, respectively. It is thus apparent that in all the results considered, the detection algorithm for voltage sags using the wavelet transform has the best performance particularly in terms of the level of accuracy.

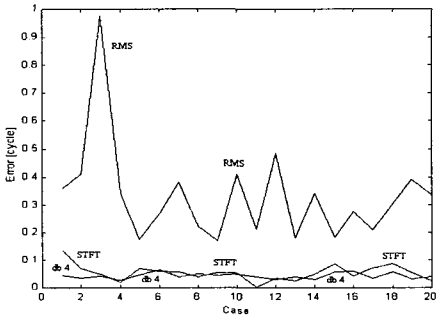

Fig. 10 Estimated error of start time

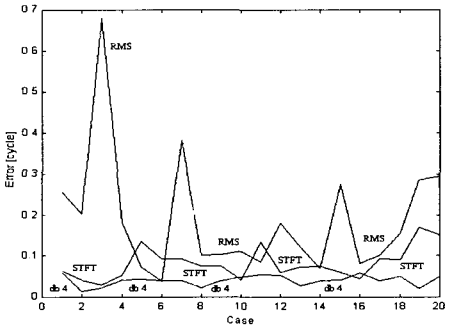

Fig. 11 Estimated error of end time

5.5 Detection Techniques for Voltage Sags Caused by a Fault

In order to simulate voltage sags caused by a fault, faults at two different points are simulated by the EMTP as shown in Fig. 12; these are listed as follows. Start times, end times and duration of each fault are 296.4 msec, 440.3 msec and 8.634 cycles, respectively, for both faults.

(1) a-earth fault on bus 32 (bus32a)
(2) a-earth fault on bus 50 (bus50a)

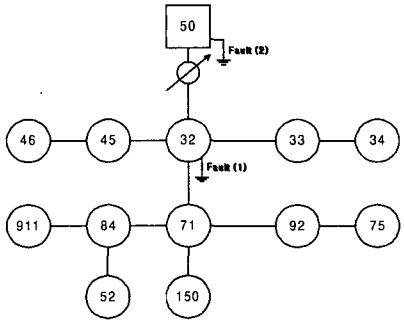

Fig. 12 Fault points in IEEE 13-bus test system

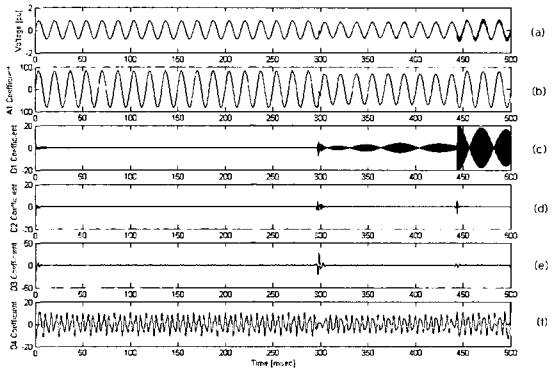

Fig. 13 Results of MRA of voltage sag at bus 34a
(a) Waveform of voltage sag
(b) A1 coefficient
(c) D1 coefficient
(d) D2 coefficient
(e) D3 coefficient
(f) D4 coefficient

In the case of a-earth fault at bus 32 (bus32a), voltage sags occur at 2 spots, namely bus 34a and bus 50a. Table 6 shows the results of detection using maximum values based on D2 coefficients, where all voltage sags caused by a-earth fault on bus 32 can be detected. Fig. 13 depicts the results of 4 levels of multiresolution analysis of voltage sag at bus34a, Fig. 13a being the input waveform of voltage sag caused by a-earth fault at bus 32. Fig. 13b is the A1 coefficient and Figs. 13c, 13d, 13e and 13f correspond to D1, D2, D3 and D4 coefficients, respectively. It is apparent from these realized waveforms that D2 is the only coefficient that explicitly provides the requisite information for the discrimination of the start and end of the voltage sag.

In the case of a-earth fault at bus 50 (bus50a), voltage sags occur at 14 spots. Here again, as in the previous case, the only suitable coefficient for accurately detecting the voltage sag (with the exception of one case) is D2; the behavior of this coefficient is summarized in Table 7, which shows the results of detection using maximum values based on D2 coefficients. Average errors of estimated start and end times are 0.165 cycle, and 0.9 cycle, respectively.

Table 6 Results of detection for voltage sags due to the fault based on D2 coefficients (a-earth fault on bus 32)

bus #	Start time		End time		RMS of A1 coeffs. [pu]	Duration time [cycle]
	Estimated time [msec]	Error [cycle]	Estimated time [msec]	Error [cycle]		
bus34c	297.1	0.0441	444.0	0.2226	0.830	8.813
bus34b	297.9	0.0910	444.0	0.2226	0.781	8.766
	Avg. error	0.0676 [cycle]	Avg. error	0.2226 [cycle]		

Table 7 Results of detection for voltage sags due to the fault based on D2 coefficients (a-earth fault on bus 50)

bus #	Start time		End time		RMS of A1 coeffs. [pu]	Duration time [cycle]
	Estimated time [msec]	Error [cycle]	Estimated time [msec]	Error [cycle]		
bus34c	300.3	0.2316	444.5	0.2539	0.848	8.656
bus34b	297.1	0.0441	298.7	8.4961	0.344	0.094
bus33b	300.3	0.2316	444.5	0.2539	0.465	8.656
bus33a	297.1	0.0441	445.3	0.3008	0.545	8.891
bus150b	300.3	0.2316	447.1	0.4101	0.390	8.813
bus46b	300.3	0.2316	444.5	0.2539	0.461	8.656
bus45b	300.3	0.2316	444.5	0.2539	0.462	8.656
bus75b	300.3	0.2316	447.1	0.4101	0.391	8.813
bus50b	297.1	0.0441	444.8	0.2695	0.565	8.859
bus50a	297.1	0.0441	445.6	0.3164	0.563	8.906
bus32a	297.1	0.0441	445.3	0.3008	0.545	8.891
bus32b	300.3	0.2316	444.5	0.2539	0.465	8.656
bus92b	300.3	0.2316	447.1	0.4101	0.390	8.813
bus71b	300.3	0.2316	447.1	0.4101	0.390	8.813
	Avg. error	0.1647 [cycle]	Avg. error	0.8995 [cycle]		

It should be mentioned that only a limited set of results for detection of voltage sag under fault conditions within a network as presented here. No doubt, in practice many other types of fault (including those with equipment such as transformer windings, etc.) can occur and cause voltage sags elsewhere within the network. Currently, a full-scale study involving a range of practically encountered faults is underway and the results will be presented in a subsequent paper.

6. Conclusions

In this paper, a novel detection technique for voltage sags using the wavelet transform has been proposed. In addition, the most appropriate mother wavelet in detecting voltage sags i.e. db4 mother wavelet, is suggested. The proposed algorithm is compared with other methods based on STFT and RMS voltage. Its validity is demonstrated with simulation studies in relation to the IEEE 13-bus test system including modeling of voltage sags caused by change of linear loads in the EMTP software.

Results from the simulation studies show that the analysis and the algorithm developed are accurate and effective compared to the more traditional approaches, under various voltage sags in distribution lines. It is proposed to extend the work not only to detect but also to classify various types of disturbances automatically.

Finally, the limited study presented also shows the capability of the technique to satisfactorily detect voltage sags under fault conditions.

Acknowledgements

This work has been supported by EESRI(02340), which is funded by MOCIE(Ministry of commerce, industry and energy).

References

[1] M.B. Hughes, J.S. Chan, "Canadian National Power Quality Survey," *in Proc. 12th International Conference on Electricity Distribution*, IEE Conference Publication No. 373, 1993.

[2] R.C. Dugan, M.F. McGranaghan, H.W. Beaty, *Electrical Power Systems Quality*, McGraw–Hill, 1996.

[3] Math H. Bollen, *Understanding Power Quality Problems*, IEEE Press, 1999.

[4] M.J. Samotyj, "Voltage Sag in Industrial Systems," *IEEE Trans. Industry Applications*, vol. 29, no. 2, pp. 397-403, March, 1993,.

[5] A.C. Parsons, W.M. Grady, E.J. Powers, "A Wavelet-Based Procedure for Automatically Determining the Beginning and End of Transmission System of Voltage Sags," *in IEEE PES Winter Meeting '99*, vol. 2, pp. 1310-1315, 1999.

[6] P.F. Ribeiro, "Wavelet Transform: An Advanced Tool for Analyzing Non-Stationary Harmonic Distortions in Power Systems," *in Proc. of the IEEE International Conference on Harmonics in Power Systems*, Bologna, pp. 365-369, September, 1994.

[7] O. Poisson, P. Rioual, M. Meunier, "New Signal Processing Tools Applied to Power Quality Analysis," *IEEE Trans. Power Delivery*, vol. 14, no. 2, pp. 561-566, April, 1999.

[8] C.H. Kim, R.K. Aggarwal, "Wavelet Transforms in Power Systems," *Power Engineering Journal*, vol. 14, no. 2, pp. 81-87, April, 2000.

[9] N.S.D. Brito, "Daubechies Wavelets in Quality of Electrical Power," *in Proc. ICHQP '98*, pp. 511-515, 1998.

[10] G.T. Heydt, "Transient Power Quality Problems Analyzed using Wavelets," *IEEE Trans. Power Delivery*, vol. 12, no. 2, pp. 908-915, April, 1997.

[11] S. Santos, E.J. Powers, W.M. Grady, P. Hofmann, "Power Quality Assessment via Wavelet Transform Analysis," *IEEE Trans. Power Delivery*, vol. 11, no. 2, pp. 924-930, April, 1996.

[12] D.C. Robertson, I. Octavia, Camps, J.S. Mayer, W.B. Gish, "Wavelet and Electromagnetic Power System Transients," *IEEE Trans. Power Delivery*, vol. 11, no. 2, pp. 1050-1058, April, 1996.

[13] S.J. Huang, C.T. Hsieh, C.L. Huang, "Application of Morlet Wavelets to Supervise Power System Disturbance," *IEEE Trans. Power Delivery*, vol. 14, no. 1, pp.235-243, January, 1999.

[14] J. Liu, P. Pillay, "An Insight into Power Quality Disturbance using Wavelet Transform Multiresolution Analysis," *IEEE Power Engineering Review*, vol. 19, no. 9, pp. 59-60, September, 1999.

[15] IEEE Distribution Planning Working Group Report, "Radial Distribution Test Feeders," *IEEE Trans. Power Systems*, vol. 6, no. 3, pp. 975-985, August, 1991.

Young-Hun Ko
He received B.S degree in Electrical Engineering and M.S degree in Electrical and Computer Engineering from Sungkyunkwan University, Korea, in 1998 and 2000, respectively. He has been working as a Researcher of the product R&D center at Daewoo Computer.

Chul-Hwan Kim (MIEEE)
He received B.S and M.S degrees in Electrical Engineering from Sungkyunkwan University, Korea, 1982 and 1984, respectively. He received a Ph.D in Electrical Engineering from Sungkyunkwan University in 1990. In 1990 he joined Cheju National University, Cheju, Korea, as a Full-time Lecturer. He was a Visiting Academic at the University of BATH, UK, in 1996, 1998 and 1999. Since March 1992, he has been a Professor in the School of Electrical and Computer Engineering, Sungkyunkwan University, Korea. His research interests include power system protection, artificial intelligence application for protection and control, modeling /protection of underground cable and EMTP software.

Sang-Pil Ahn
He received B.S degree in Electrical Engineering and M.S degree in Electrical and Computer Engineering from Sungkyunkwan University, Korea, in 1997 and 1999, respectively. He has been working as a Researcher at the Korea Electro-technology Research Institute.